LOWLAND TECHNOLOGY INTERNATIONAL Vol. 8, No. 1, 37-46, June 2006
International Association of Lowland Technology (IALT), ISSN 1344-9656

DEFORMATION BEHAVIOR OF SHIRASU SOIL BY THE EXTENDED SUBLOADING SURFACE MODEL

M. Hira[1], K. Hashiguchi[2], M. Ueno[3] and T. Okayasu[4]

ABSTRACT: This study is aimed at evaluation of the deformation behavior of *Shirasu* soil (volcanic sandy soil) for reclamation and embankment construction, using elastoplastic constitutive equation based on the subloading surface model with the rotational hardening. Test results for isotropic consolidation and monotonic/cyclic loading-unloading compression with several lateral stresses under the drained conditions for various initial void ratios are reported. Further, the simulation by the constitutive equation based on the extended subloading surface model is compared with the test results. High applicability of the constitutive equation for the prediction of mechanical behavior of Shirasu soil for a geo-material at the lowland in the southern Kyushu is verified by the comparison.

Keywords: Constitutive equation, subloading surface model, Shirasu soil, stress-strain relation, elasto-plasiticity

INTRODUCTION

Volcanic sandy soil *Shirasu* is widely distributed in the neighboring parts of Caldera in Southern Kyushu, Japan. It has considerable apparent cohesion in the undisturbed state as a soft rock but loses cohesion in the disturbed state as sand, whilst the disturbance is caused even by a submersion. Shirasu is generally used as a geo-material at the construction sites for reclamation and embankment construction, etc. around the costal areas in Kagoshima. Hence, the prediction of the deformation behavior of this soil is of importance from the viewpoint of practical engineering. Triaxial test results have been reported by Haruyama (1969, 1977, 1985, 1987) revealing the shear characteristics, the angle of internal friction, failure condition, etc. However, the prediction of stress-strain relation for Shirasu by elastoplastic constitutive equations has not been reported so far, although a number of research papers on the deformation behavior of Shirasu have been published in the past. Here, it is noteworthy that elastoplastic constitutive equation has been highly developed in recent years. Particularly, the subloading surface model (Hashiguchi and Ueno, 1977; Hashiguchi, 1978; Hashiguchi, 1980; Hashiguchi and Chen, 1998) falling within the framework of the *unconventional plasticity* (Drucker 1988) in which the interior of yield surface is not assumed to be an elastic domain. It would be applicable to the description of the deformation behavior of soils in not only the normally-consolidated but also in the over-consolidated states to which Shirasu usually belongs, whilst the Cambridge theory (Roscoe and Burland 1968), (Schofield and Wroth 1968) is applicable only to the description of deformation behavior in the normal-consolidated state.

In this article the prediction of the deformation behavior of Shirasu by the elastoplastic constitutive equation is investigated introducing the subloading surface model with the rotational hardening (Hashiguchi 1994, 2001; Hashiguchi and Chen 1998; Hira et al. 2002).

Besides, test results for the isotropic consolidation and the triaxial monotonic and cyclic compression loading under drained conditions for normal- and over-consolidated states for various initial void ratios subjected to various levels of lateral stress are described in detail. Further, the calculated results by the constitutive equation are compared with the test results. High ability of the constitutive equation for the prediction of mechanical behavior of Shirasu is shown as the results of simulation.

[1] Research Associate, Faculty of Agriculture, Kagoshima University, Korimoto 1-21-24,Kagoshima 890-0065, JAPAN
[2] Professor, Graduate School of Kyushu University, Hakozaki 6-10-1, Higashi-ku, Fukuoka 812-8581, JAPAN
[3] Professor, Faculty of Agriculture, University of the Ryukyus, Senbaru 1, Nishihara, Okinawa 903-0213, JAPAN
[4] Associate Professor, Graduate School of Kyushu University, Hakozaki 6-10-1, Higashi-ku, Fukuoka 812-8581, JAPAN
Note: Discussion on this paper is open until December 31, 2006

SUBLOADING SURFACE MODEL

In this section the subloading surface model (Hashiguchi 1994, 2001), (Hashiguchi and Chen 1998) and its application to soils is reviewed briefly, and will be latter applied to the analysis of the deformation behavior of Shirasu. Let it be assumed that the stretching $\mathbf{D}$ is additively decomposed into the elastic stretching $\mathbf{D}^e$ and the plastic stretching $\mathbf{D}^p$, i. e.

$$\mathbf{D} = \mathbf{D}^e + \mathbf{D}^p \tag{1}$$

where the elastic stretching $\mathbf{D}^e$ is given by

$$\mathbf{D}^e = \mathbf{E}^{-1} \overset{\circ}{\boldsymbol{\sigma}} \tag{2}$$

$\boldsymbol{\sigma}$ is the *Cauchy stress* and $(^\circ)$ indicates the proper corotational rate with the objectivity (e.g. Dafalias 1985, Zbib and Aifantis 1988) and the fourth-order tensor E is the elastic modulus given in the Hooke's type as,

$$E_{ijkl} = (K - \frac{2}{3}G)\delta_{ij}\delta_{kl} + G(\delta_{ik}\delta_{jl} + \delta_{il}\delta_{jk}) \tag{3}$$

where K and G are the bulk and shear moduli, respectively, which are functions of stress and internal state variables in general and δ_{ij} is the Kronecker's delta, i. e. $\delta_{ij} = 1$ for $i = j$ and $\delta_{ij} = 0$ for $i \neq j$.

Normal-yield and Subloading Surfaces

Let the following yield condition be assumed.

$$f(\boldsymbol{\sigma}, \boldsymbol{\beta}) = F(H) \tag{4}$$

where the second-order tensor $\boldsymbol{\beta}$ is the inherent or induced anisotropic hardening variable and the scalar H is the isotropic hardening/softening variable. Let it be assumed that the function f is homogeneous of degree one in $\boldsymbol{\sigma}$, satisfying $f(t\boldsymbol{\sigma}, \boldsymbol{\beta}) = tf(\boldsymbol{\sigma}, \boldsymbol{\beta})$ for any nonnegative scalar t. The inherent and the induced anisotropy of soils can be described concisely by the *rotational hardening*, whilst the kinematic hardening is inapplicable to soils as has been described by Hashiguchi (2001).

Let the *subloading surface* (Hashiguchi and Ueno, 1977; Hashiguchi, 1978;Hashiguchi, 1980; Hashiguchi and Chen, 1998) be introduced, which always passes through the current stress $\boldsymbol{\sigma}$ and keeps the similarity to the normal-yield surface with respect to the origin of stress space, i. e. $\boldsymbol{\sigma} = 0$. Besides, the ratio of the size of the subloading surface to that of the normal-yield surface will be denoted by R which can be regarded as the

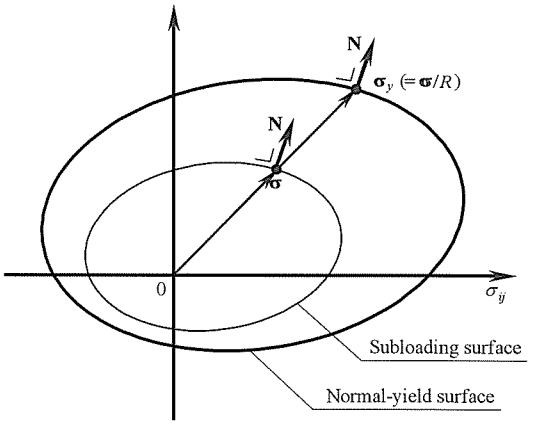

Fig. 1 Normal-yield and subloading surfaces

measure of approaching degree to the normal-yield state and is thus called the *normal-yield ratio*. The conjugate stress $\boldsymbol{\sigma}_y$ on the normal-yield surface for the current stress $\boldsymbol{\sigma}$ on the subloading surface due to the similarity is given by

$$\boldsymbol{\sigma}_y = \frac{\boldsymbol{\sigma}}{R} \tag{5}$$

By substituting Eq. (5) into Eq. (4) with regarding $\boldsymbol{\sigma}$ in Eq. (4) as $\boldsymbol{\sigma}_y$, the subloading surface is described as

$$f(\boldsymbol{\sigma}, \boldsymbol{\beta}) = RF(H) \tag{6}$$

The normal-yield and the subloading surfaces are illustrated in Fig. 1.

Plastic Stretching

The time-differentiation of Eq. (6) for the subloading surface is given by

$$\mathrm{tr}\left(\frac{\partial f(\boldsymbol{\sigma}, \boldsymbol{\beta})}{\partial \boldsymbol{\sigma}} \overset{\circ}{\boldsymbol{\sigma}}\right) - \mathrm{tr}\left(\frac{\partial f(\boldsymbol{\sigma}, \boldsymbol{\beta})}{\partial \boldsymbol{\beta}} \overset{\circ}{\boldsymbol{\beta}}\right) = \dot{R}F + RF'\dot{H} \tag{7}$$

where

$$F' \equiv \frac{dF}{dH} \tag{8}$$

$\mathrm{tr}(\ )$ denotes the trace and $(^\bullet)$ stands for the material-time derivative. $\dot{H}$ is given by

$$\dot{H} = f_H(\boldsymbol{\sigma}, \mathbf{D}^p) \tag{9}$$

where the function f_H is homogeneous of degree one in the plastic stretching $\mathbf{D}^p$ since $\dot{H}$ has minus one dimension of time and satisfies $\dot{H} = 0$ for $\mathbf{D}^p = 0$.

Taking account of the fact that a stress asymptotically approaches the normal-yield surface, i. e. that the subloading surface approaches the yield surface in the plastic loading process, let the evolution rule of the normal-yield ratio R be given by

$$\dot{R} = U_R \left\| \mathbf{D}^p \right\| \text{ for } \mathbf{D}^p \neq \mathbf{0} \tag{10}$$

where U_R is the monotonically decreasing function of R, satisfying

$$\left.\begin{array}{ll} U_R = +\infty & \text{for } R = 0, \\ U_R = 0 & \text{for } R = 1, \\ (U_R < 0 & \text{for } R > 1). \end{array}\right\} \tag{11}$$

as illustrated in Fig. 2. $\| \ \|$ stands for the magnitude, i.e. $\|\mathbf{T}\| = \sqrt{\mathrm{tr}(\mathbf{T}\mathbf{T}^{\mathrm{T}})}$. The function U_R satisfying Eq. (11) be given by

$$U_R = -u \ln R \tag{12}$$

where u is a material constant.

Substituting Eq. (10) into Eq. (7), one has the *extended consistency condition* for the subloading surface:

$$\mathrm{tr}\left(\frac{\partial f(\boldsymbol{\sigma},\ \boldsymbol{\beta})}{\partial \boldsymbol{\sigma}} \overset{\circ}{\boldsymbol{\sigma}}\right) - \mathrm{tr}\left(\frac{\partial f(\boldsymbol{\sigma},\ \boldsymbol{\beta})}{\partial \boldsymbol{\beta}} \overset{\circ}{\boldsymbol{\beta}}\right) = U_R \left\| \mathbf{D}^p \right\| F + RF'\dot{H} \tag{13}$$

Assume the *associated flow rule* for the subloading surface

$$\mathbf{D}^p = \lambda \mathbf{N} \ (\lambda > 0) \tag{14}$$

where λ is the proportionality factor and the second-order tensor N is the normalized outward-normal of the subloading surface, i.e.

$$\mathbf{N} \equiv \frac{\partial f(\boldsymbol{\sigma},\ \boldsymbol{\beta})}{\partial \boldsymbol{\sigma}} \Big/ \left\| \frac{\partial f(\boldsymbol{\sigma},\ \boldsymbol{\beta})}{\partial \boldsymbol{\sigma}} \right\| \tag{15}$$

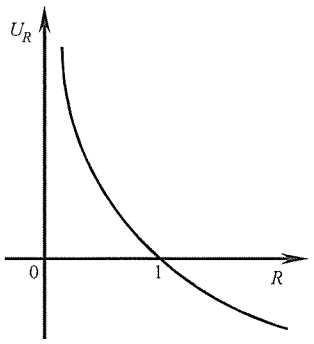

Fig. 2 Function U_R of the variable R

The substitution of Eq. (14) into the extended consistency condition (13) leads to

$$\lambda = \frac{\mathrm{tr}(\mathbf{N}\overset{\circ}{\boldsymbol{\sigma}})}{M_p} \tag{16}$$

where

$$M_p \equiv \left\{ \frac{F'}{F} h + \frac{U_R}{R} + \frac{1}{RF} \mathrm{tr}\left(\frac{\partial f(\boldsymbol{\sigma},\ \boldsymbol{\beta})}{\partial \boldsymbol{\beta}} \mathbf{b} \right) \right\} \mathrm{tr}(\mathbf{N}\boldsymbol{\sigma}) \tag{17}$$

h and b are the scalar and the tensor functions of the stress, plastic internal state variables and N in degree one, which is related to $\dot{H}$ and $\overset{\circ}{\boldsymbol{\beta}}$ as

$$h \equiv \frac{\dot{H}}{\lambda}, \ \mathbf{b} \equiv \frac{\overset{\circ}{\boldsymbol{\beta}}}{\lambda} \tag{18}$$

since $\dot{H}$ and $\overset{\circ}{\boldsymbol{\beta}}$ includes λ in degree one.

The plastic stretching is obtained from Eqs. (14) and (16) as

$$\mathbf{D}^p = \frac{\mathrm{tr}(\mathbf{N}\overset{\circ}{\boldsymbol{\sigma}})}{M_p} \mathbf{N} \tag{19}$$

The stretching is obtained from Eqs. (1), (2) and (19) as

$$\mathbf{D} = \mathbf{E}^{-1} \overset{\circ}{\boldsymbol{\sigma}} + \frac{\mathrm{tr}(\mathbf{N}\overset{\circ}{\boldsymbol{\sigma}})}{M_p} \mathbf{N} \tag{20}$$

The positive proportionality factor in the associated flow rule (14) is expressed in terms of the stretching **D**, rewriting λ by Λ, as follows:

$$\Lambda = \frac{\mathrm{tr}(\mathbf{NED})}{M_p + \mathrm{tr}(\mathbf{NEN})} \tag{21}$$

The inverse expression of Eq. (20) is obtained from Eqs. (1), (2), (14) and (21) as

$$\overset{\circ}{\boldsymbol{\sigma}} = \mathbf{ED} - \frac{\mathrm{tr}(\mathbf{NED})}{M_p + \mathrm{tr}(\mathbf{NEN})} \mathbf{EN} \tag{22}$$

Loading Criterion

The loading criterion is given as follows (Hill 1958, 1967):

$$\left.\begin{array}{l} \mathbf{D}^p \neq \mathbf{0}: \ \mathrm{tr}(\mathbf{NED}) > 0, \\ \mathbf{D}^p = \mathbf{0}: \ \mathrm{tr}(\mathbf{NED}) \leq 0 \end{array}\right\} \tag{23}$$

which is applicable not only to the hardening state but also to the perfectly-plastic and the softening states.

The plastic stretching (19) is obtained by substituting the associated flow rule (14) into the extended consistency condition (13) which is obtained by incorporating the evolution rule (10) of the normal-yield ratio R into the time-differentiation of Eq.(7) for the subloading surface. The plastic deformation develops gradually as the stress approaches the normal-yield surface, exhibiting a *smooth elastic-plastic transition*. Thus, the subloading surface model fulfills the *smoothness condition* (Hashiguchi 1993a, 1993b, 1997, 2000) defined as "the stress rate-stretching relation (or the stiffness tensor) changes continuously for a continuous change of stress state", which can be expressed mathematically as follows:

$$\lim_{\delta\boldsymbol{\sigma}\to\mathbf{0}}\frac{\partial\mathring{\boldsymbol{\sigma}}(\boldsymbol{\sigma}+\delta\boldsymbol{\sigma},\mathbf{S}_i,\mathbf{D})}{\partial\mathbf{D}}=\frac{\partial\mathring{\boldsymbol{\sigma}}(\boldsymbol{\sigma},\mathbf{S}_i,\mathbf{D})}{\partial\mathbf{D}} \tag{24}$$

where $\mathbf{S}_i$ (i=1, 2, 3, …, m) denotes collectively scalar- or tensor-valued internal state variables describing the alteration of mechanical response property due to the irreversible deformation, $\delta(\ )$ stands for an infinitesimal variation and the response of the stress rate to the stretching in the current state of stress and internal variables is designated by $\mathring{\boldsymbol{\sigma}}(\boldsymbol{\sigma},\mathbf{S}_i,\mathbf{D})$.

Formulation of Extended Subloading Surface Model and Material Functions for Shirasu

Based on the equations formulated in previous section, the kinematic hardening variable α and the similarity-center $\boldsymbol{s}$ are introduced to the initial subloading surface model in this section.

Let the stress function in Eq. (6) of the subloading surface be given for soils as

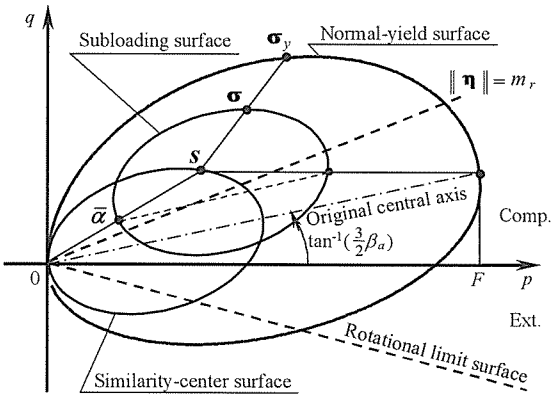

Fig. 3 Normal-yield and subloading surfaces for Shirasu with the rotational hardening

$$f(\boldsymbol{\sigma},\boldsymbol{\beta})=p\{1+\left(\frac{\|\hat{\boldsymbol{\eta}}\|}{\hat{m}}\right)^2\} \tag{25}$$

where

$$p\equiv-\frac{1}{3}\mathrm{tr}\boldsymbol{\sigma},\ \hat{\boldsymbol{\eta}}\equiv\frac{\boldsymbol{\sigma}^*}{p}-\boldsymbol{\beta},\boldsymbol{\sigma}^*\equiv\bar{\boldsymbol{\sigma}}+p\mathbf{I} \tag{26}$$

$$\bar{\boldsymbol{\sigma}}=\boldsymbol{\sigma}-\bar{\boldsymbol{\alpha}},\ \bar{\boldsymbol{\alpha}}=\boldsymbol{s}-R(\boldsymbol{s}-\boldsymbol{\alpha}) \tag{27}$$

$(\ )^*$ stands for the deviatoric component. The second-order tensor $\boldsymbol{\beta}$ is taken as the *rotational hardening variable*, i.e. the rotation of yield surface, advocated by Sekiguchi and Ohta (1977), whilst $\boldsymbol{\beta}$ is fixed in their formulation. The evolution equation of $\boldsymbol{\beta}$ has been given by Hashiguchi (1994) and Hashiguchi and Chen (1998) as follows:

$$\mathring{\boldsymbol{\beta}}=b_r\|\mathbf{D}^{p*}\|\|\hat{\boldsymbol{\eta}}\|(m_r\frac{\hat{\boldsymbol{\eta}}}{\|\hat{\boldsymbol{\eta}}\|}-\boldsymbol{\beta}) \tag{28}$$

b_r is the material constants and m_r is the stress ratio exhibiting the limitation of the rotation of yield surface, whilst the surface $\|\boldsymbol{\eta}\|=m_r$ is called the *rotational-limit surface* which is the function of

$$\sin3\theta_\sigma\equiv-\sqrt{6}\frac{\mathrm{tr}\boldsymbol{\eta}^3}{\|\boldsymbol{\eta}\|^3} \tag{29}$$

m_r is given by

$$m_r=\frac{2\sqrt{6}\sin\phi_r}{3-\sin\phi_r\sin3\theta_\sigma} \tag{30}$$

where ϕ_r is referred to the friction angle for the rotational-limit surface under the axisymmetric stress state. The rotational-limit surface with Eq. (30) exhibits the conical surface satisfying the Coulomb-Mohr failure surface at the axisymmetric stress state. On the other hand, $\hat{m}$ is the stress ratio in the critical state and is a function of

$$\sin3\hat{\theta}_\sigma\equiv-\sqrt{6}\frac{\mathrm{tr}\hat{\boldsymbol{\eta}}^3}{\|\hat{\boldsymbol{\eta}}\|^3} \tag{31}$$

Here, $\hat{m}$ is given as

$$\hat{m}=\frac{2\sqrt{6}\sin\phi}{3-\sin\phi\sin3\hat{\theta}_\sigma} \tag{32}$$

where ϕ is referred to the frictional angle in the critical state under the axisymmetric stress state. The normal-yield and the subloading surfaces with the rotational hardening for soils are illustrated in Fig. 3 where q is the

deviatoric stress, i.e. $q \equiv \sigma_a - \sigma_l$ (σ_a : axial stress, σ_l : lateral stress) and σ_a is the axial component of $\boldsymbol{\beta}$.

And the evolutional rule of the similarity-center is obtained as follows:

$$\mathring{\boldsymbol{s}} = c\left\|\mathbf{D}^p\right\|\frac{\tilde{\boldsymbol{\sigma}}}{R} + \mathring{\boldsymbol{\alpha}} + \left\{\dot{F}\text{-tr}\left(\frac{\partial f(\boldsymbol{s},\mathbf{H})}{\partial \mathbf{H}}\mathring{\mathbf{H}}\right)\right\}\boldsymbol{s} \tag{33}$$

where c is the material constant.

The isotropic hardening/softening function F is given by

$$F = F_0 \exp\left(\frac{H}{\rho - \gamma}\right) \tag{34}$$

where F_0 is the initial value of F which is taken so as to coincide with the normal-consolidation pressure p_y. ρ and γ are material constants describing the inclinations of the normal-consolidation and the swelling lines, respectively, in the $(\ln v,\ \ln p)$ plane (v: volume) illustrated in Fig. 4 (Hashiguchi 1995). The rate of the isotropic hardening/softening variable H is given by $\dot{H} = -D_v^p$, where D_v^p ($\equiv \mathrm{tr}\mathbf{D}^p$) is the plastic volumetric strain. The elastic bulk and shear moduli are given as $K = p/\gamma$, $G = 3\mathrm{K}(1-2\nu)/2(1+\nu)$ (ν ; Poisson's ratio).

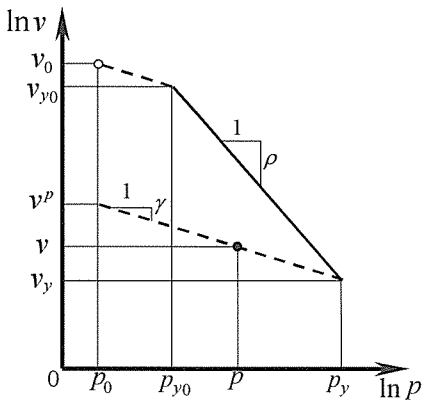

Fig. 4 Linear relation of ln$p$ versus ln$v$ for isotropic consolidation of soils

COMPARISON WITH TEST DATA

Sample Properties and Testing Procedure

Shirasu sample used for the tests was taken from Mizobe-cho, Kagoshima Prefecture. The physical properties are shown in Table 1. The gravel fraction of Shirasu consists mainly of pumice and a small amount of derived rock fragments such as andesite. The particles are considerably angular. Coarse fragments are subangular to angular, and the shape becomes angular as the grain size becomes finer, and only thin, flat and angular particles are observed in the finest fraction. Most of the fragments are volcanic glass; its surface texture generally looks smooth. On the other hand, the pumice has frothy structure and its surface is very rough. This is the reason why the Shirasu has small density compared with other sandy soils. The water content was adjusted to be 15% after natural drying in the laboratory and sieving through a sieve of 2 mm meshes. The specimens were compacted using a rammer in a cylindrical mold of 50 mm in diameter and 125 mm in height, so as to give a specified initial density. Furthermore, the layer and compaction numbers were set in accordance with the form of Proctor's equation to give three kinds of density, and thus initial void ratio was prepared to be three levels 0.83, 0.95 and 1.01. At the specimen preparation stage, attention was paid to the adjustment of initial void ratio by the compaction method in order to realize a precise comparison of test results depending on the difference of initial void ratio.

In order to measure volumetric change precisely, nearly saturated specimens (Skempton's B-value > 0.95) are prepared by vacuum procedure (Rad and Clough 1984) in which the effective isotropic stress $\boldsymbol{\sigma}$ =4.9 I kPa (0.05 kgf/cm^2) is applied to specimens at the beginning of tests. Then, the isotropic loading-unloading tests and the conventional triaxial compression tests were performed by the stress/strain control. In case of the isotropic consolidation process the small pressure increments of 4.9 kPa are added in stages by the computer-aided control such that a volume change negligible in each stage taking more than ten minutes. On the other hand, in case of the axial compression tests the small axial strain rate of 0.1 %/min. is added so as not to cause the excess pore pressure in the drained tests with four levels of confining pressure 98 (1), 196 (2), 294 (3) and 392 (4) kPa (kgf/cm^2), whilst axial loads at the maximum level of 196 kPa under total confining pressure 98 kPa are applied to samples for the cyclic loading-unloading tests.

Table 1 Physical properties of Shirasu

Grading	Sand	77	%
	Silt	20	%
	Clay	3	%
Coefficient of uniformity	U_c	38.9	
Coefficient of curvature	U_c'	3.84	
Specific gravity of soil particles	G_s	2.43	

Material Parameters for Simulation

The material constants ρ, γ and the initial value F_0 are determined so as to fit the test result of isotropic consolidation illustrated in Fig. 5. The Poisson's ratio ν is obtained by the value of γ and the inclination of the initial rising part of stress-strain curve in the triaxial compression test results. The parameter u in the evolution rule of the normal-yield ratio R is determined from the curvature of the stress-strain curve in the transitional state from the elastic to the normal-yield state, while it is smaller for looser samples. The stress ratio at the stress on the normal-yield surface in which the outward-normal vector loses the component of hydrostatic axis changes only slightly. Especially, it is fixed independent of the rotation in the yield surface of the original Cam-clay model. The angle ϕ of internal friction in the critical state can be determined approximately from the stress ratio in the residual state. The limit-angle ϕ_r of the rotational hardening and the parameter b_r controlling the rate of rotational hardening are determined so as to supplement the degree of hardening in the test result with the deviatoric deformation. The material parameters used in the simulation are listed in Table 2, where F_0 stands for the values of F in the initial state ($\boldsymbol{\sigma}$ =4.9I kPa) of calculation.

The rotational hardening has to be incorporated in order to simulate several test data with different lateral stresses using a unique set of values of material parameters, whilst only one test datum could be simulated without adopting the rotational hardening. Besides, it is impossible to change the void ratio so much as 0.1 without the particle crushing for materials composed of large particles as sands, Shirasu, etc. by the quasi-static small deformation process. On the other hand, constitutive equations at the present level can deal only with the quasi-static small deformation process without the scattering of particles in the dynamic deformation process by which specimens with different void ratios are prepared. Besides, the relationship between material parameters and initial void ratio has not been revealed yet for sands, Shirasu, etc. The values of material parameters are given independently for the loose, the middle and the dense specimens in the model simulation.

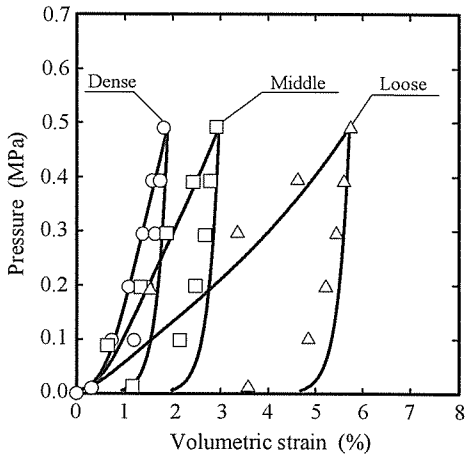

Fig. 5 Relations of volumetric strain versus pressure for isotropic loading-unloading processes

COMPARISON OF THEORY AND EXPERIMENT

All the calculations start from the unique isotropic effective stress state $\boldsymbol{\sigma}$ =4.9I kPa and thus in the triaxial tests the isotropic consolidation test is performed until

Table 2 Material parameters used for Shirasu samples

Parameters		Dense	Middle dense	Loose
Initial void ratio(average)	e_0	0.83	0.95	1.01
Initial value of hardening function	F_0	790 kPa	495 kPa	210 kPa
Internal frictional angle in the critical state	ϕ	36°	36°	36°
Evolution rate of the rotational hardening	b_r	350	300	210
Rotational limit angle	ϕ_r	23°	22°	19°
Evolution rate of the normal-yield ratio	u	65	60	50
Initial value of the similarity-center	s	70	70	70
Material constant for the move of similarity-center	c	30	30	30
Inclination of normal-consolidation line	ρ	0.040	0.042	0.047
Inclination of swelling line	γ	0.002	0.002	0.002
Poisson's ratio	ν	0.3	0.3	0.3

the prescribed confining pressure. All the calculated results are depicted by solid lines.

Isotropic loading-unloading consolidation behavior for dense, middle dense and loose samples is shown in Fig. 5. A fairly good prediction of the volumetric strain-pressure curves is attained. The differences of the volumetric strain with changes in the initial void ratio are realistically simulated by the theory, whilst the plastic deformation is predicted properly even in the subyield state.

The relationships of the deviatoric stress and the volumetric strain versus the axial strain under the drained triaxial compression are depicted in Fig. 6 for dense, middle dense and loose samples subjected to four levels of confining pressure (Fig. 6). The deviatoric stress-axial strain curves of dense samples exhibit a peak in the deviatoric stress, whilst the curvature of the curves decreases with the increment of the confining pressure. The predicted stresses after peak are higher than the stresses in the test results. It might be caused by the shear band formation in the test samples as will be described in the end of this section. On the other hand, the curves of loose samples do not exhibit a peak in spite of the confining pressure. The volumetric strain-axial strain curves also agree well with the test data. The phenomenon observed in the test results of dense samples that the maximum ratio of the volumetric strain increment to the axial strain increment is realized at the peak state of axial stress is predicted exactly by the theory. This phenomenon has been widely known as the experimental fact for over-consolidated soils as has been written even in the classical literature of Taylor (1948). It was also suggested by Newland and Alley (1957) from the micromechanical aspect that "*When sliding just begins, the shear stress and rate of volumetric expansion reach maximum values, since at this state the sliding contact angles of soil particles to the shear plane are at their maximum*". Besides, smooth stress-strain curves are predicted for monotonic loading process by the present theory, whilst a sharp bent in the stress-strain curves at the initial yield state is predicted by the conventional theory represented by the *Cambridge theory* (Roscoe and Burland, 1968; Schofield and Wroth, 1968) for normal-consolidated state and the *Drucker-Prager* (1952) for over-consolidated state.

Besides, the cyclic loading-unloading test results under the confining pressure at 98 kPa are shown in Fig. 7. All parameters are the same as those of monotonic loading tests for each initial density. A good prediction of the strain-stress curves is attained, whilst the hysteresis behavior of stress-stain curve for soils is realistically described and the accumulation of strain by calculation is provided. The stress-strain tendencies by

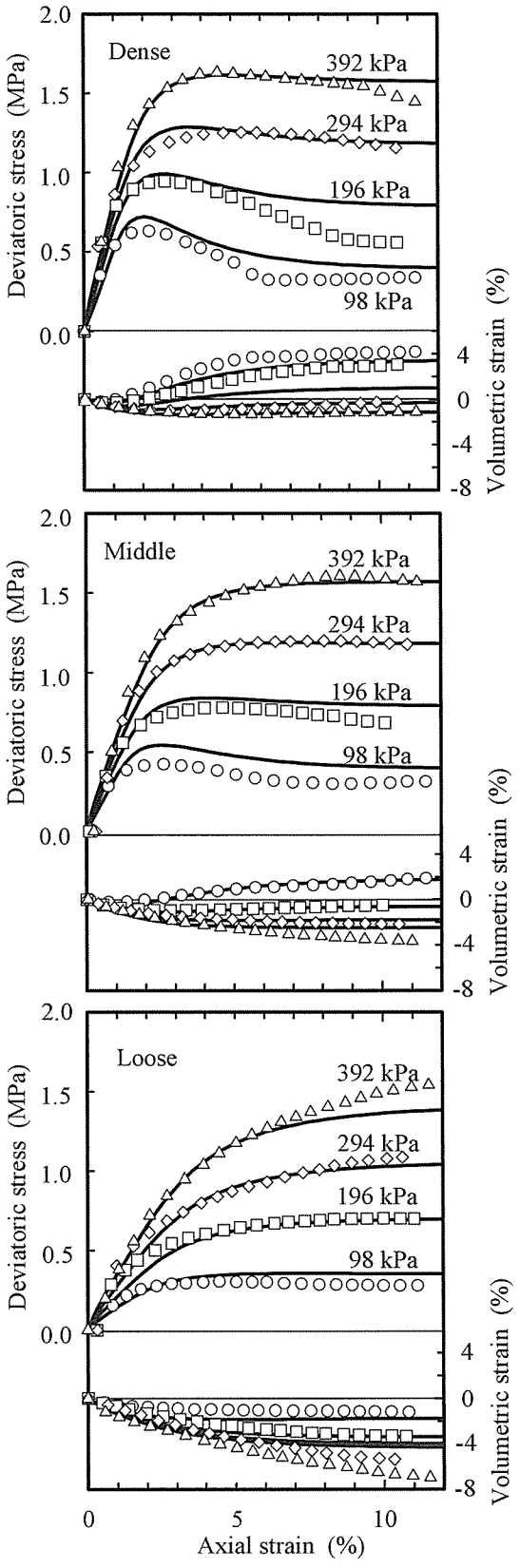

Fig. 6 Relations of axial strain versus deviatoric stress, axial strain versus volumetric strain for drained triaxial compression test of dense, middle and loose samples

simulation results are verified by comparison with the cyclic loading-unloading tests. It is shown that the application of the extended subloading surface concept is very useful to consider the cyclic loading problems. In this article the parameters are examined to be identical by the initial density (initial void ratio).

MECHANICAL FEATURES OF SHIRASU SOIL

The deformation behavior of compacted Shirasu is predicted here by the elastoplastic constitutive equation. The prediction has been attained historically first in this paper. Therefore, it is difficult yet to found mechanical features of Shirasu definitely. In the present situation the following mechanical features of Shirasu from the viewpoint of constitutive equation might be indicated as compared to those of clays (Topolnicki, 1990; Asaoka et al., 1997; Hashiguchi, 2001) and sands (Hashiguchi and Chen, 1998; Noda et al., 2001).

1. Particles of Shirasu have size similar to that of sands but are quite angular leading to cohesion by compaction. Therefore, in general, Shirasu exhibits deformation behavior of clays and/or sands depending on the test conditions. Besides, the compacted Shirasu sample exhibits rather brittle behavior and thus would lead to shear band formation causing an apparent softening more intense than softening predicted as a constitutive property. It would be the reason for the difference of stress-strain curves after peak stress in calculated and test results and prediction as seen in Fig. 6.

2. After the initial unloading stage, the value of axial strain is very small as shown is Fig.7, the plastic strain component of Shirasu is also small.

3. The void ratio is large in the order of clays, Shirasu and sands, and thus ρ (inclination of normal-consolidation line) is larger (easily compressed and fragile) and evolution rate of the normal-yield ratio u in Eq. (12) is smaller (easily deforms plastically) as in above order.

4. The elastic deformation is substantially caused by the deformation of soil particles themselves, and thus inclination of swelling (elastic consolidation) curve γ is not so different between clays, Shirasu and sands.

CONCLUSIONS

The description of deformation behavior of Shirasu soil by the elastoplastic constitutive equation is studied adopting the subloading surface model with the rotational hardening. The predicted results by the

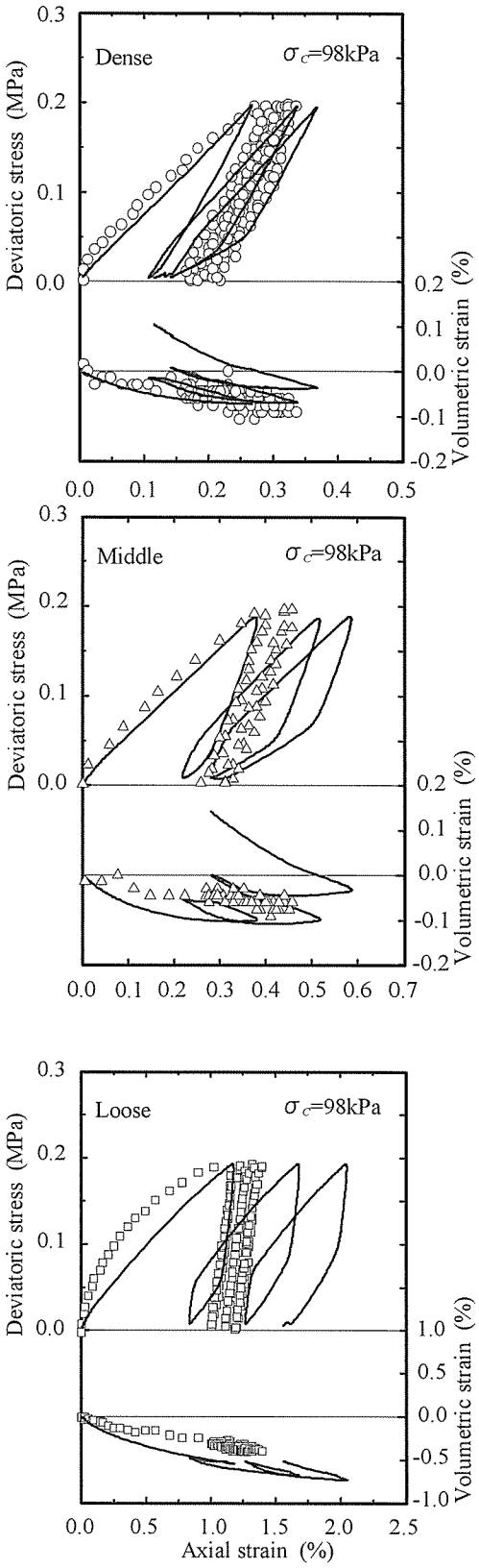

Fig. 7 Relations of axial strain versus deviatoric stress, axial strain versus volumetric strain for cyclic loading-unloading test under drained condition

constitutive equation were compared with some test data of compacted Shirasu samples for the isotropic consolidation and the triaxial monotonic and cyclic compression under the drained condition for normal- and over-consolidated states for various initial void ratios subjected to various levels of lateral stress. Calculations were performed starting from unique isotropic stress state and using each unique set of values of material parameters depending on dense, middle and loose samples. The capability of reproducing real deformation behavior of this volcanic sandy soil was verified in this comparison.

Further, the constitutive equation is limited to the prediction of monotonic loading behavior. In order to predict the cyclic loading behavior of Shirasu, the extended subloading surface model with kinematic hardening variable can be shown to be in good agreement with test results. The elastoplastic constitutive equation using the extension of the subloading surface model is effective in predicting a mechanical ratcheting behavior for soils. However, tested samples are limited to artificially compacted samples and thus the comparison with undisturbed natural samples would be desirable in order to confirm the capability.

REFERENCES

Asaoka, A., Nakano, M. and Noda, T. (1997). Soil-water coupled behavior of heavily overconsolidated clay near/at critical state. Soils and Foundations, 37 (1):13-28.

Dafalias, Y.F. (1985). The plastic spin. J. Appl. Mech. (ASME), 52:865-871.

Drucker, D.C. and Prager, W. (1952). Soil mechanics and plastic analysis or limit design. Quart. Appl. Math, 10:157-164.

Drucker, D.C. (1988). Conventional and unconventional plastic response and representation. Appl. Mech. Rev. (ASME), 41:151-167.

Haruyama, M. (1969). Effect of water content on the shear characteristics of granular soils such as Shirasu. Soils and Foundations, 9 (3): 35-57.

Haruyama, M. (1977). Deformation characteristics of highly compressible sand "Shirasu". Soils and Foundations, 17 (1): 39-51.

Haruyama, M. (1985). Drained deformation-strength characteristics of loose Shirasu (volcanic sandy soil) under three dimensional stresses. Soils and Foundations, 25 (1): 65-76.

Haruyama, M. (1987). Effect of density on the drained deformation behavior of Shirasu (volcanic sandy soil) under three-dimensional stresses. Soils and Foundations, 27 (1):1-13.

Hashiguchi, K. (1978). Plastic constitutive equations of granular materials. Proc. US-Japan Seminar Continuum Mech. Stast. Appr. Mech. Granular Materials, Sendai: 321-329.

Hashiguchi, K. (1980). Constitutive equations of elastoplastic materials with elastic-plastic transition. J. Appl. Mech. (ASME), 47:266-272.

Hashiguchi, K. (1993a). Mechanical requirements and structures of cyclic plasticity models. Int. J. Plasticity, 9:721-748.

Hashiguchi, K. (1993b). Mechanical requirements and structures of cyclic plasticity models. Int. J. Plasticity, 9: 721-748.

Hashiguchi, K. (1994). Subloading surface model with rotational hardening. Proc. Int. Conf. Compt. Meth. Struct. Geotech. Eng., Hong Kong: 807-812.

Hashiguchi, K. (1995). On the linear relation of V-lnp and lnv-lnp for isotropic consolidation of soils. Int. J. Numer. Anal. Meth. Geomech., 19:367-376.

Hashiguchi, K. (1997). The extended flow rule in plasticity. Int. J. Plasticity, 13: 37-58.

Hashiguchi, K. (2000). Fundamentals in constitutive equation: continuity and smoothness conditions and loading criterion. Soils and Foundations, 40 (3): 155-161.

Hashiguchi, K. (2001). Description of inherent/induced anisotropy of soils: Rotational hardening rule with objectivity. Soils and Foundations, 41 (6):139-145.

Hashiguchi, K. and Chen, Z.-P. (1998). Elastoplastic constitutive equation of soils with the subloading surface and the rotational hardening. Int. J. Numer. Anal. Mech. Geomech., 22:197-227.

Hashiguchi, K. and Ueno, M. (1977). Elastoplastic constitutive laws of granular materials, Constitutive Equations of Soils. (Proc. 9th ICFSME, Spec. Sess. 9), Tokyo, JSSMFE, Tokyo:73-82.

Hill, R. (1958). A general theory of uniqueness and stability in elastic-plastic solids. J. Mech. Phys. Solids, 6: 236-249.

Hill, R. (1967). On the classical constitutive relations for elastic/plastic solids, Recent Progress Appl. Mech. (The Folke Odqvist Volume). John Wiley & Sons: 241-249.

Hira, M., Hashiguchi, K., Okayasu, T. and Miwa, K. (2002). Deformation Behavior of "Shirasu" and Its Prediction by the Subloading Surface Model. Soils and Foundations, 42(5):37-46.

Newland, P.L. and Alley, B.H. (1957). Volume changes in drained triaxial tests on granular materials. Geotechnique, 7: 17-32.

Noda, T., Nakano, M., Mizuno, K. and Takeuchi, H. (2001). A soil-water coupled analysis on the effect of improvement of a loose sandy ground by cylindrical cavity expansion. Soils and Foundations, 41 (4):113-123. (in Japanese)

Rad, N.S. and Clough, G.W. (1984). New procedure for saturating sand specimens. J. Geo. Eng. Div. (ASCE), 110: 1205-1218.

Roscoe, K.H. and Burland, J.B. (1968). On the generalized stress-strain behavior of 'wet' clay. Engineering Plasticity (eds. Heyman, J. and Leckie, F.A.), Cambridge Univ. Press: 535-608.

Schofield, A.N. and Wroth, C.P. (1968). Critical State Soil Mechanics. McGraw-Hill. London.

Sekiguchi, H. and Ohta, H. (1977). Induced anisotropy and time dependency in clays. Constitutive Equations of Soils (Proc. 9th ICFSME, Spec. Session 9), Tokyo, JSSMFE, Tokyo: 229-238.

Taylor, D.W. (1948). Fundamentals of soil mechanics. John Wiley, New York: 329-359.

Topolnicki, M. (1990). An elasto-plastic subloading surface model for clay with isotropic and kinematic mixed hardening parameters. Soils and Foundations, 30 (2):103-113.

Zbib, H.M. and Aifantis, E.C. (1988). On the concept of relative and plastic and its implications to large deformation theories. Part I: Hypoelasticity and vertex-type plasticity. Acta. Mech., 75: 15-33.